



Force-closure workspace analysis of cable-driven parallel mechanisms

Cong Bang Pham ^{a,*}, Song Huat Yeo ^a, Guilin Yang ^b,
Mustafa Shabbir Kurbanhusen ^a, I-Ming Chen ^a

^a School of Mechanical and Aerospace Engineering, Nanyang Technological University, Singapore 637098, Singapore

^b Mechatronics Group, Singapore Institute of Manufacturing Technology, Singapore 638075, Singapore

Received 9 November 2004; received in revised form 23 March 2005; accepted 27 April 2005

Available online 27 June 2005

Abstract

A cable-driven parallel mechanism (CDPM) possesses a number of promising advantages over the conventional rigid-link mechanisms, such as simple and light-weight mechanical structure, high-loading capacity, and large reachable workspace. However, the formulations and results obtained for the rigid-link mechanisms cannot be directly applied to CDPMs due to the unilateral property of cables. This paper focuses on the workspace analysis of fully restrained positioning mechanisms. Because the cable tension is the most essential issue to constrain the moving platform, the force-closure workspace is mainly studied. A general approach is proposed to check the force-closure condition. This condition is expressed in terms of the convex hull which encloses the origin. However, such a condition is formulated and expressed in high dimensions. To simplify the analysis, a recursive dimension reduction algorithm is proposed to check convex hulls in one dimension spaces. This algorithm is verified through simulation results of various CDPMs. © 2005 Elsevier Ltd. All rights reserved.

Keywords: Force-closure; Workspace analysis; Cable-driven mechanism

* Corresponding author.

E-mail addresses: pa0146775b@ntu.edu.sg (C.B. Pham), myeosh@ntu.edu.sg (S.H. Yeo), glyang@simtech.a-star.edu.sg (G. Yang), must0003@ntu.edu.sg (M.S. Kurbanhusen), michen@ntu.edu.sg (I-Ming Chen).

1. Introduction

Currently, most of mechanisms used for robot manipulators are conventional linkage mechanisms that consist of a number of rigid links and joints. Based on their kinematic structures, these mechanisms are classified into two major types: serial and parallel mechanisms [1]. Fig. 1 shows a cable-driven parallel mechanism (CDPM) formed by replacing all the supporting legs of a parallel mechanism with cables. It is seen that the CDPM is a closed-loop mechanism in which the moving platform is connected to the base by several cables. The base suspending points can be mounted at the extremities of the base. Therefore, these manipulators can perform manipulation tasks requiring a large reachable workspace. Generally, a CDPM has the following significant advantages:

- Simple light-weight mechanical structure, resulting in low energy consumption.
- Large reachable workspace, limited mainly by cable lengths and cable tension constraints.
- Low moment inertia and high speed motion.
- Easy reconfigurability by relocating platform connecting points and base suspending points.

The advantages make the CDPM a promising alternative to the rigid-link mechanisms in many industrial applications, such as load lifting and positioning [2], coordinate measurement [3,4], aircraft testing [5], haptic devices [6,7], and robot rehabilitation [8].

Unlike rigid links, cables are characterized by the unilateral property (can pull but cannot push moving platforms), and therefore the formulations and results obtained for the kinematics analysis, workspace analysis, trajectory planning, etc. of the rigid-link mechanisms cannot be directly applied. Hence, one challenging issue is to determine the poses whereby the moving platform is fully constrained by the cables. For CDPMs, it is known that maintaining positive cable tension is critical in constraining the moving platform. Hence, the force-closure workspace of CDPMs is a set of poses whereby resultant cable tensions can sustain an arbitrary external wrench acting on the moving platform. Once the force-closure workspace is obtained, its area (in planar cases) or its

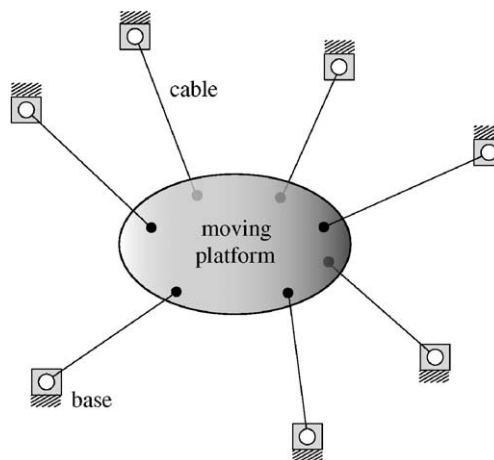


Fig. 1. A cable-driven parallel mechanism.

volumes (in spatial cases) can be used as a primary criteria to design a cable-driven parallel mechanism such that the force-closure workspace matches the required workspace.

Because of the advantages and unique features of cables, CDPMs have received a great attention in robotics literature. The first general classification was given by Ming and Higuchi [9]. Based on the number of cables (m) and the number of degrees of freedom (n), the CDPMs were classified into three categories, i.e. the incompletely restrained positioning mechanisms ($m < n + 1$), the completely restrained positioning mechanisms ($m = n + 1$) and the redundantly restrained positioning mechanisms ($m > n + 1$). With such classification, a number of different workspaces have been studied. One of the early works is that for the NIST ROBOCRANE [2], which is similar to a Gough–Stewart platform parallel manipulator, but replacing the parallel links with a number of cables. Tadokoro also analyzed the reachable workspace for a cable-driven, six-DOF motion base for virtual sensation of acceleration [10], and explored the reachable workspace of a redundant eight-wire mechanism to derive optimal wire configuration [11]. Dynamic workspace analysis has been performed by Gosselin and Barrette [12] in such a way that the motion of a moving platform is incorporated into a set of wrenches called a *pseudo-pyramid*. The statically reachable workspace is defined by Agrawal and coworkers [13] as the set all end-effector poses that can be reached statically. Additionally, Verhoeven et al. has explored the controllable workspace and other workspace properties for tendon based Stewart platforms in [14–16]. Recently, Ebert–Uphoff has reviewed some basic workspace terminologies for cable-driven robots [17] and also geometrically explored the wrench-feasible workspace for cable-driven robots by visualizing a net wrench set as a hyper-parallelogram [18]. A similar research issue termed the cable-force region is also explored by Osumi et al. [19]. However, in constraining positive cable tensions, these analyses are almost based on the null space approach through pseudo-inverse matrices or graphical approaches that are only convenient in some specific cases.

The objectives of this paper are to develop a general algorithm to examine the force-closure condition which is sufficient to fully restrain the moving platform, and to generate the force-closure workspace for CDPMs. Here, the research is focused on fully restrained CDPMs ($m \geq n + 1$). A general recursive approach is proposed to check the force-closure condition. This condition is expressed in terms of the convex hull which encloses the origin. Recursivity implies that checking the convex hull is realized in $(n - 1)$ -dimensional spaces instead of in an n -dimensional space. This is done by reducing one row and one column of the original system at a time via Gaussian eliminations. This algorithm is verified through applying it to analyze the workspace of both the completely restrained 4-3 cable-driven planar parallel mechanism (4-3-CDPPM) as shown in Fig. 2(a) and the redundantly restrained 8-6 cable-driven spatial parallel mechanism (8-6-CDSPM) as shown in Fig. 2(b).

In our analysis, the following assumptions are made:

- Each motor controls the length of exactly one cable; therefore, there are m motors and m cables.
- Due to the fact that cables can only pull but cannot push, all cables must remain in positive tension at all times.
- All cables are assumed to be inelastic and extend in straight line paths from the base suspending point B_i to the platform connecting point P_i .

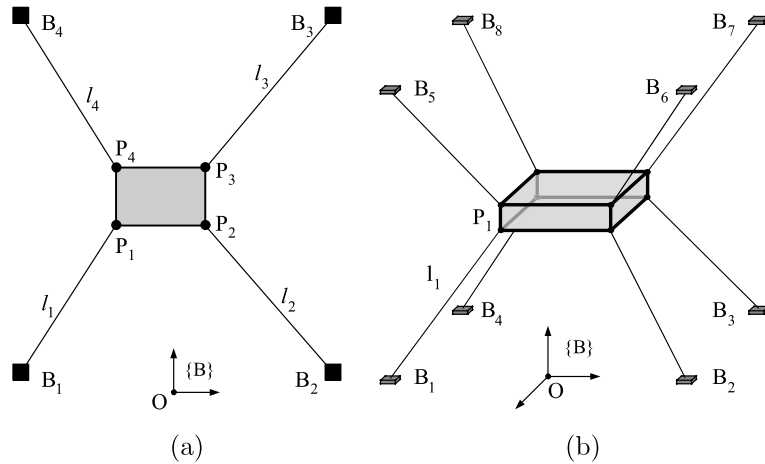


Fig. 2. Two examples of symmetric cable-driven parallel mechanisms: (a) 4-3-CDPPM: completely restrained positioning mechanism, (b) 8-6-CDSPM: redundantly restrained positioning mechanism.

The remaining sections of this paper are organized as follows: in Section 2, kinematic modelling and static equilibrium of the moving platform are formulated. Force-closure condition and recursive convex hull checking algorithm followed by force-closure workspace generation are presented in Section 3. Section 4 illustrates some results of force-closure workspace obtained by the recursive algorithm. The paper is summarized in Section 5.

2. Kinematic modelling and static equilibrium

A schematic diagram of a fully restrained CDPM is shown in Fig. 3, in which the moving platform is connected to the base through driving cables, $l_i = \overrightarrow{B_i P_i} (i = 1, 2, \dots, m)$.

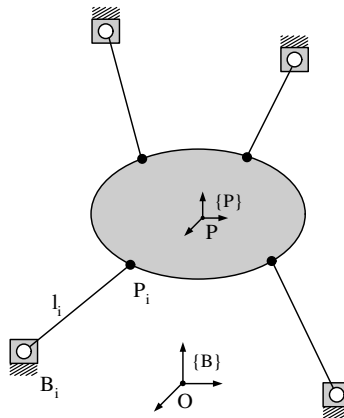


Fig. 3. Kinematic diagram of a CDPM.

Let frame $\{B\}$ be the base frame and frame $\{P\}$ be the moving platform frame (attached at the center of mass P of the moving platform). The frame $\{P\}$ is known with respect to the frame $\{B\}$ by the kinematic transformation matrix $\mathbf{T}_{B,P}$ as follows:

$$\mathbf{T}_{B,P} = \begin{bmatrix} \mathbf{R} & \mathbf{p} \\ \mathbf{0} & 1 \end{bmatrix} \quad (1)$$

where $\mathbf{p} = \{x \ y \ z\}^T$ is the position vector of point P with respect to the base frame $\{B\}$ and

$$\mathbf{R} = \begin{bmatrix} c\alpha \cdot c\beta & (-s\alpha \cdot c\gamma + c\alpha \cdot s\beta \cdot s\gamma) & (s\alpha \cdot s\gamma + c\alpha \cdot s\beta \cdot c\gamma) \\ s\alpha \cdot c\beta & (c\alpha \cdot c\gamma + s\alpha \cdot s\beta \cdot s\gamma) & (-c\alpha \cdot s\gamma + s\alpha \cdot s\beta \cdot c\gamma) \\ -s\beta & c\beta \cdot s\gamma & c\beta \cdot c\gamma \end{bmatrix}$$

represents the orientation of frame $\{P\}$ with respect to frame $\{B\}$, in which α , β and γ are the $Z - Y - X$ Euler angles [20].

In order to sustain any external wrench $(\mathbf{f}_p, \mathbf{m}_p)$ applied on the moving platform, all cables must be able to create tension forces to achieve equilibrium of the moving platform. Referring to Fig. 4, the equilibrium conditions for force and torque at the moving platform are as follows:

$$\sum_{i=1}^m \mathbf{t}_i + \mathbf{f}_p = \mathbf{0} \quad (2)$$

$$\sum_{i=1}^m \mathbf{r}_i \times \mathbf{t}_i + \mathbf{m}_p = \mathbf{0} \quad (3)$$

where $\mathbf{t}_i = t_i \mathbf{u}_i = -t_i \frac{\mathbf{l}_i}{l_i}$ represents the tension force that acts in the opposite direction of \mathbf{l}_i . Substituting \mathbf{t}_i into Eqs. (2) and (3), the following equation is obtained:

$$\mathbf{A} \cdot \mathbf{T} = \mathbf{B} \quad \text{with } \mathbf{T} \geq 0 \quad (4)$$

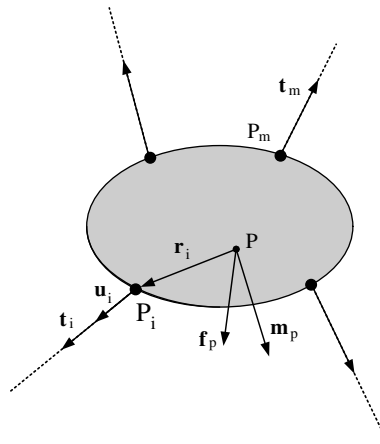


Fig. 4. Free body diagram of the moving platform.

where

$$\mathbf{A} = \begin{bmatrix} \mathbf{u}_1 & \mathbf{u}_2 & \cdots & \mathbf{u}_m \\ \mathbf{r}_1 \times \mathbf{u}_1 & \mathbf{r}_2 \times \mathbf{u}_2 & \cdots & \mathbf{r}_m \times \mathbf{u}_m \end{bmatrix} \in \mathbb{R}^{n \times m} : \text{structure matrix}$$

$$\mathbf{T} = \{t_1 \ t_2 \ \cdots \ t_m\}^T \in \mathbb{R}^m : \text{cable tension}$$

$$\mathbf{B} = -\{\mathbf{f}_p \ \mathbf{m}_p\}^T \in \mathbb{R}^n : \text{external wrench}$$

The directional unit vector \mathbf{u}_i ($i = 1, 2, \dots, m$) in the structure matrix depends on the posture of the moving platform and is obtained by the vector loop-closure equation as:

$$\mathbf{u}_i = \frac{\overrightarrow{OB_i} - \overrightarrow{OP} - \overrightarrow{PP_i}}{\|\overrightarrow{OB_i} - \overrightarrow{OP} - \overrightarrow{PP_i}\|} = \frac{\mathbf{b}_i - \mathbf{p} - \mathbf{R}\mathbf{r}_i^p}{\|\mathbf{b}_i - \mathbf{p} - \mathbf{R}\mathbf{r}_i^p\|} \quad (5)$$

where the superscript p is used to denote that the quantity is written in frame $\{P\}$. Hence, the structure matrix \mathbf{A} is expressed with respect to the posture of the moving platform.

3. Force-closure workspace

For parallel mechanisms with rigid links, its workspace is the space where the inverse/forward kinematic solutions exist. However for a CDPM, its workspace is the space where sets of positive cable tensions exist because they are needed to constrain the moving platform all the time regardless of any external wrench. In other words, if there is at least one set of positive cable tensions at a specific pose forming a force closure, then this pose belongs to the force-closure workspace. Generally, force-closure workspace is a set of poses that the force-closure condition is satisfied.

3.1. Force-closure condition

A CDPM is said to have a force-closure in a particular pose if and only if any arbitrary external wrench applied at the moving platform can be sustained through appropriate tension forces (t_1, t_2, \dots, t_m) in the cables. With the assumption that the actuator torques are of unlimited magnitude, from Eq. (4), the condition of being fully restrained is mathematically described as

$$\forall \mathbf{F}_p \in \mathbb{R}^n : \exists t_1, t_2, \dots, t_m \in [0, \infty) : \sum_{i=1}^m t_i \mathbf{s}_i = -\mathbf{F}_p \quad (6)$$

where $\mathbf{s}_i = \begin{Bmatrix} \mathbf{u}_i \\ \mathbf{r}_i \times \mathbf{u}_i \end{Bmatrix}$: the i th column vector of the structure matrix \mathbf{A} .

Eq. (6) implies that the set of vectors $t_i \mathbf{s}_i$ must positively span \mathbb{R}^n . Subsequently, this set is positively dependent (by choosing $\mathbf{F}_p = 0$) such that:

$$\text{rank}(\mathbf{A}) = n \text{ and} \quad (7)$$

$$\sum_{i=1}^m t_i \mathbf{s}_i = 0 \quad (8)$$

From the convex theory [21], the following theorem shows that the set of all convex combinations in the left hand side of Eq. (8) is actually a convex hull.

Theorem 1. Let $C = \{\mathbf{x}_1, \mathbf{x}_2, \dots, \mathbf{x}_m\}$ be a finite collection of points in \mathbb{R}^n . Then the convex hull of the \mathbf{x}_i ($i = 1, 2, \dots, m$), is the set of all their convex combinations, i.e.

$$H = \text{co}(C) = \left\{ \mathbf{x} \mid \mathbf{x} = \sum_{i=1}^m \lambda_i \mathbf{x}_i, \quad \sum_{i=1}^m \lambda_i = 1, \quad 0 \leq \lambda_i \in \mathbb{R} \text{ for all } i \right\}$$

Eq. (8) is equivalently represented as follows:

$$\sum_{i=1}^m t_i \mathbf{s}_i = \sum_{i=1}^m \frac{t_i}{\sum_{i=1}^m t_i} \mathbf{s}_i = \sum_{i=1}^m \lambda_i \mathbf{s}_i = \mathbf{0} \quad \text{with } \lambda_i = \frac{t_i}{\sum_{i=1}^m t_i} \quad (9)$$

From the notation of Theorem 1, Eq. (9) forms a convex hull based on the structure matrix \mathbf{A} . Furthermore, the origin belongs to that convex hull because the origin is the convex combination of \mathbf{s}_i . Hence, the following proposition shows an utilization of convex hull in satisfying the force-closure condition.

Proposition 1. A moving platform with n degrees of freedom is fully restrained if and only if the convex hull formed by column vectors of the structure matrix \mathbf{A} , $\text{co}\{\mathbf{s}_1, \mathbf{s}_2, \dots, \mathbf{s}_m\}$, contains a neighborhood of the origin.

Proof. *Necessity:* Because the platform is fully restrained, a small external wrench $O(\varepsilon)$ can be expressed by Eq. (6) such that:

$$\sum_{i=1}^m t_i \mathbf{s}_i = O(\varepsilon) \quad (10)$$

Dividing Eq. (10) by $\sum_{i=1}^m t_i$ gives:

$$\sum_{i=1}^m \frac{t_i}{\sum_{i=1}^m t_i} \mathbf{s}_i = \frac{O(\varepsilon)}{\sum_{i=1}^m t_i} \simeq O(\varepsilon) \quad (11)$$

It is obvious that the neighborhood of the origin belongs to the convex hull (according to Theorem 1).

Sufficiency: As the neighborhood of the origin $O(\varepsilon)$ is enclosed by the convex hull, it can be expressed:

$$\sum_{i=1}^m t_i \mathbf{s}_i = O(\varepsilon) \quad \text{with } \sum_{i=1}^m t_i = 1 \quad \text{and } \forall t_i > 0 \quad (12)$$

Eq. (12) implies that there always exists a set of positive tensions being able to sustain a small external wrench in any direction. Therefore, the moving platform is fully restrained. \square

3.2. Recursive algorithm checking force-closure condition

As discussed above, the force-closure condition is satisfied if the n -dimensional convex hull, formed by the structure matrix, encloses the origin. However, if the number of task-space dimensions n is greater than three, it is impossible to represent the convex hull geometrically. Therefore,

a general algorithm is proposed to check whether the moving platform, at a particular pose, is fully restrained. In other words, it is whether the convex hull encloses the origin of the task-space frame.

To solve the above problem in general, the resulted idea is that if the size of the task-space dimension can be reduced into one ($n = 1$), i.e. the convex hull becomes a closed line segment, it is easier to check the origin enclosure, i.e. whether this line segment passes the origin as illustrated in Fig. 5. Therefore, the dimension reduction of a structure matrix \mathbf{A} (n rows, m columns) is described in two steps as follows:

- *Step 1:* For each column vector in a space of \mathbb{R}^n , there is a unique hyperplane passing through the origin and being orthogonal to this vector. This hyperplane is a subspace of \mathbb{R}^{n-1} . By projecting the other column vectors onto this hyperplane, projected vectors are expressed in this new subspace of \mathbb{R}^{n-1} . In addition, the vector which is perpendicular to this hyperplane can be ignored due to its zero projected value. Therefore, there are only $m - 1$ column vectors in the subspace of \mathbb{R}^{n-1} . Totally, from the original space in \mathbb{R}^n , this step results in m subspaces in \mathbb{R}^{n-1} formed corresponding to m column vectors.
- *Step 2:* For each subspace formed above, there are only $m - 1$ column vectors. Therefore, the convex hull which is formed by these $m - 1$ vectors is also required to enclose the origin of the subspace in order to have a force-closure. Generally, m new convex hulls are checked for satisfaction of force-closure. If all of them encloses the origin of the respective subspaces, the original system forms a force-closure. Otherwise, if any of them does not have the force-closure, this means that a certain external wrench cannot be resisted in this subspace. Consequently, the original problem does not satisfy the force-closure condition.

These procedures are illustrated in Fig. 6. It can be seen from Fig. 6(a) that if the three vectors ($\overrightarrow{OS_i}$) are projected onto the line which is perpendicular to any vector $\overrightarrow{OS_i}$, there always exist both positive components and negative components. This means that any external force can be resisted by some of these cable tensions. On the other hand, as shown in Fig. 6(b), if the three vectors are projected onto the line which is perpendicular to $\overrightarrow{OS_1}$ or $\overrightarrow{OS_3}$, all components have the same sign. This means that all cable tensions cannot resist the external force in the same direction on the projected line. For both cases, the original convex hulls are in the space of \mathbb{R}^2 . When projected onto the line, the original problem is equivalent to three new convex hulls which are expressed as line segments in the subspace of \mathbb{R}^1 . As a result, checking force closure in the space of \mathbb{R}^1 is simple as it only involves checking the sign of components.

As mentioned in previous discussion, the first step is to reduce the space dimension and the second step is to check the convex hulls formed in the subspaces. If the dimension of the subspaces is

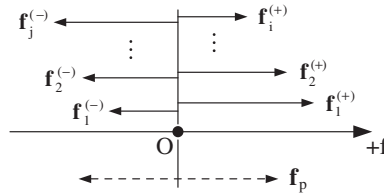


Fig. 5. $\text{Co}(f_1^{(-)}, f_1^{(+)}, \dots, f_j^{(-)}, f_i^{(+)})$ is a closed line segment passing the origin.

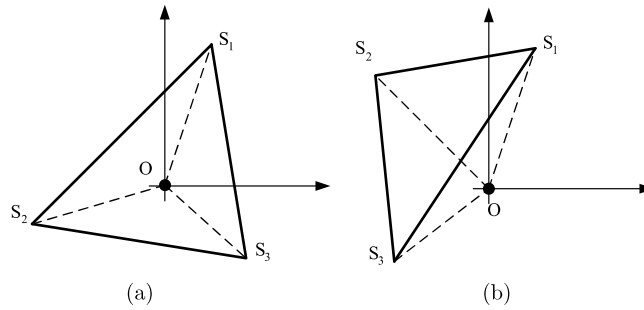


Fig. 6. Two samples of convex hull. (a) $O \in \text{co}(S_1, S_2, S_3)$. (b) $O \notin \text{co}(S_1, S_2, S_3)$.

more than one, these subspaces are further reduced into other subspaces by repeating step 1 and so on. As shown in Fig. 7, one original system in \mathbb{R}^n is decomposed to m subsystems in \mathbb{R}^{n-1} . Then each subsystem in \mathbb{R}^{n-1} is decomposed to $(m-1)$ subsystems in \mathbb{R}^{n-2} . Therefore, using more cables considerably increases the number of subsystems in \mathbb{R}^1 . Typically, for a 4-3-CDPPM, the number of subsystems in \mathbb{R}^1 is 12 whereas that for a 8-6-CDSPM is 6720.

Mathematically, it is noted that projecting column vectors onto a hyperplane which is perpendicular to the column vector j is a Gaussian elimination for the corresponding column vector. As a result, a convex hull checking procedure is proposed that is based on a recursive algorithm. This algorithm is named “FCC[$A(n, m)$]” (Force-Closure Check). Generally, by giving the original structure matrix A (n rows, m columns) to the algorithm, this algorithm will reduce the space continuously until all subspaces are one-dimensional. The flowchart of this algorithm is described in Fig. 8.

As shown in Fig. 8, the recursive algorithm FCC consists of two procedures:

- *One-dimension case:* This is the simplest case in which
 - (a) There is at least one row consisting of the same sign components. This implies that the convex hull does not enclose the origin. The algorithm returns a value ‘0’, or

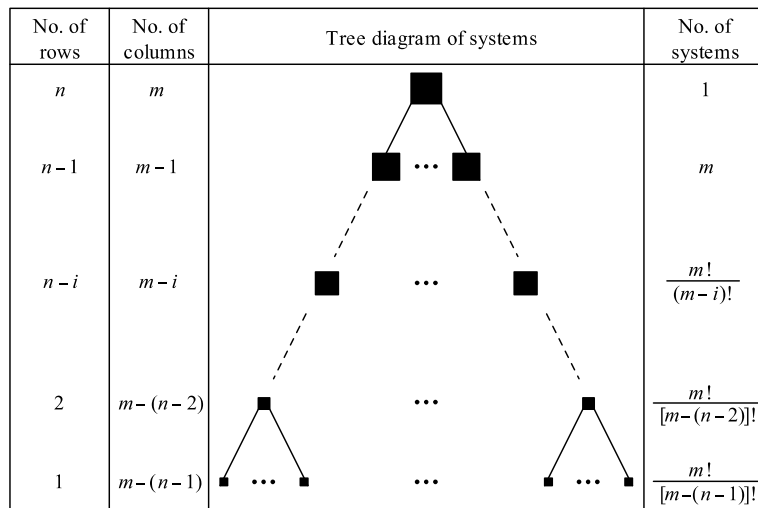


Fig. 7. Diagram of decomposing space dimension.

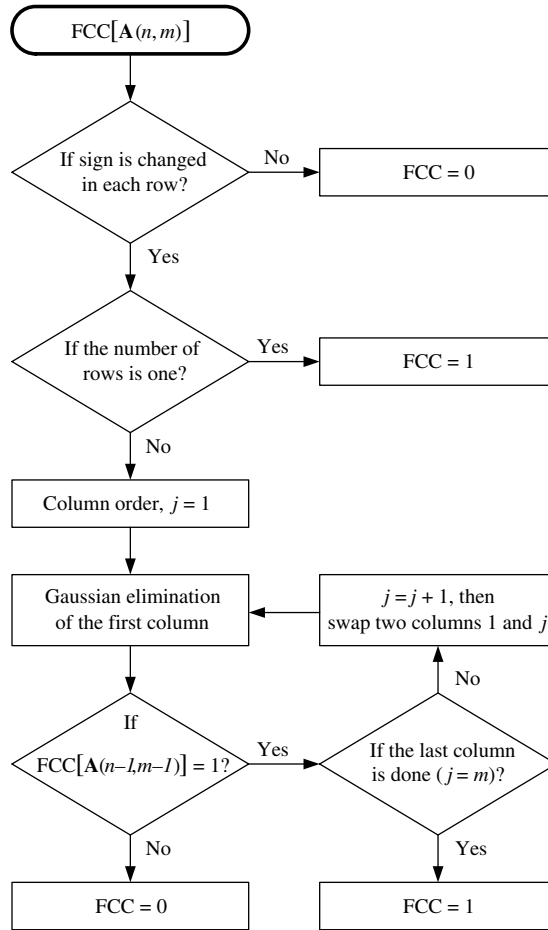


Fig. 8. Recursive algorithm “force-closure check”—FCC.

(b) The number of rows is one. If the signs among components are changed, the line segment encloses the origin. The algorithm returns a value ‘1’. Otherwise, it returns a value ‘0’, i.e. the signs are unchanged.

- *Higher dimension case:* This is the case such that the number of rows is greater than one and the signs are changed in each row. Reducing space dimension is done by Gaussian elimination until one-dimensional systems. If there is one subsystem which does not satisfy the force-closure condition, the algorithm returns a value ‘0’.

For convenient programming in Matlab, the Gaussian elimination is always done for the first column. Therefore, a column index j is used to increase the column order, then this column is swapped with the first column. To demonstrate this algorithm, detailed checking steps of two examples shown in Fig. 6 are presented in Appendix A.

3.3. Generating force-closure workspace

In formulating the force-closure workspace, a set of fully restrained postures needs to be obtained. Positional and rotational ranges are discretized into segments. At each of their combinations, a corresponding structure matrix \mathbf{A} is determined. By applying the force-closure algorithm, returning value ‘1’ means this posture belongs to the force-closure workspace, and returning value ‘0’ implies this posture does not belong to the force-closure workspace. Although this workspace generation takes time to finish, this approach is very simple and effective to obtain the workspace area or volume when necessary. If the resolution is large enough, its area or its volume is closed to analytical results which are difficult to calculate for general cable-driven parallel mechanisms.

In this paper, two typical mechanisms are used to verify the recursive force-closure algorithm. Firstly, the algorithm is applied to the completely restrained cable-driven planar parallel mechanism (3 degrees of freedom, 4 cables). For this mechanism, the orientation of the platform is fixed, a set of positions (x, y) of the center of mass of the moving platform P defines the force-closure workspace. Secondly, the algorithm is applied to the redundantly restrained cable-driven spatial parallel mechanism (6 degrees of freedom, 8 cables). Similarly, the three orientations are kept constant, and the force-closure workspace is defined by the set of positions (x, y, z) of the center of mass of the moving platform P .

4. Simulation and results

In this section, the recursive force-closure algorithm is applied to generate the force-closure workspace for the two typical mechanisms shown in Fig. 2. Simulated results shows the effect of the recursive algorithm.

In the following illustrations, the mechanisms have the symmetric design. For the planar mechanism shown in Fig. 9(a), the base is a square of 1×1 (m), and the moving platform is a rectangle that has the dimension of 0.3×0.2 (m). For the spatial mechanism shown in Fig. 9(b), the base is a unit cube of $1 \times 1 \times 1$ (m), and the moving platform is a parallelepiped that has the dimension of $0.3 \times 0.2 \times 0.1$ (m). The base frame is located at the point B_1 . The coordinates of vertices are described in Fig. 9. The local frame is located at the center P of the rectangle (in the planar case) and

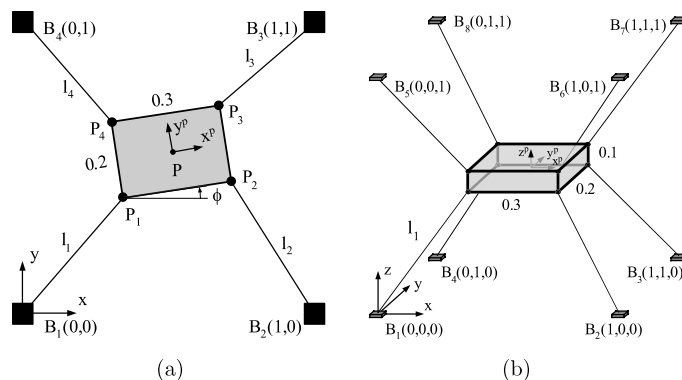
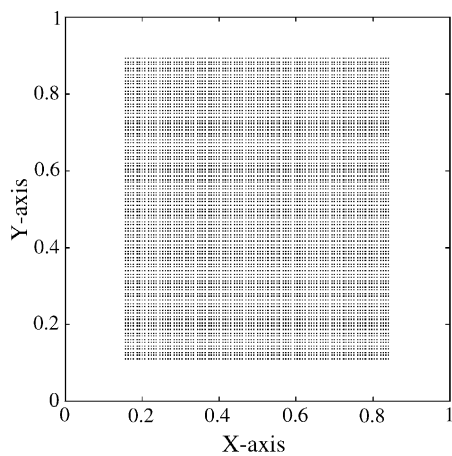
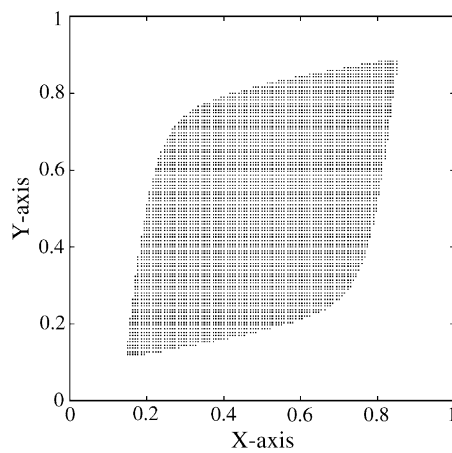


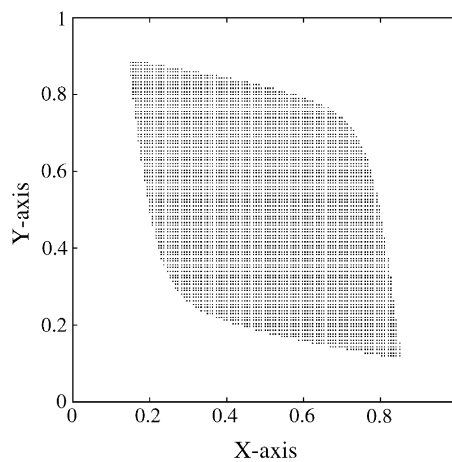
Fig. 9. Geometrical parameters. (a) A symmetric 4-3-CDPPM and (b) A symmetric 8-6-CDSPM.



(a)

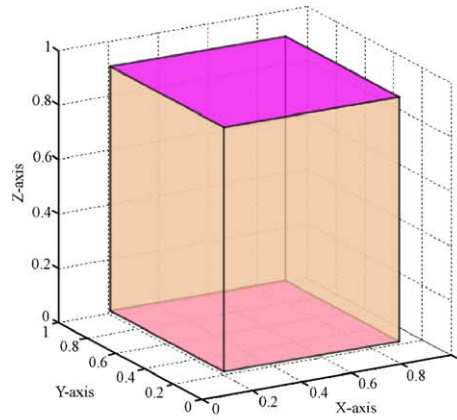


(b)

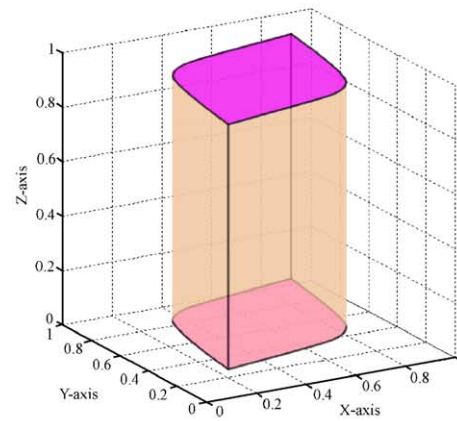


(c)

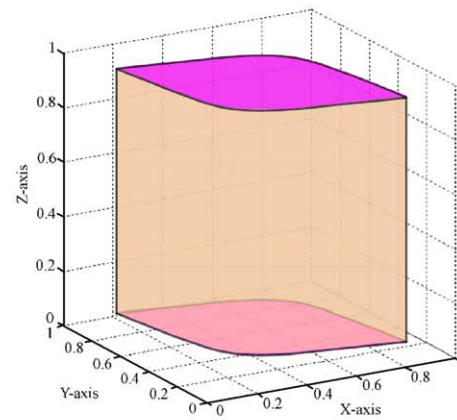
Fig. 10. Two-dimensional force-closure workspaces of the 4-3-CDPPMs. (a) $\phi = 0^\circ$, (b) $\phi = +3^\circ$ and (c) $\phi = -3^\circ$.



(a)



(b)



(c)

Fig. 11. Three-dimensional force-closure workspaces of the 8-6-CDSPM. (a) $\alpha = 0^\circ$, $\beta = 0^\circ$, $\gamma = 0^\circ$, (b) $\alpha = +3^\circ$, $\beta = 0^\circ$, $\gamma = 0^\circ$ and (c) $\alpha = -3^\circ$, $\beta = 0^\circ$, $\gamma = 0^\circ$.

of the cube (in the spatial case). Therefore, a set of reachable positions of this center P at a certain orientation of the moving platform constitutes the force-closure workspace.

As shown in Fig. 10, the force-closure workspace is generated at various orientations of the moving platform. The 2-dimensional workspaces obtained at $\phi = 0^\circ$, $+3^\circ$ and -3° are illustrated in Figs. 10(a)–(c), respectively.

In order to verify the validity of the recursive algorithm for redundantly restrained positioning mechanisms, the algorithm is also applied to a 8-6-CDSPM. Subsequently, the force-closure workspaces are illustrated in Fig. 11. By giving $\gamma = 0^\circ$ (the orientation about x) and $\beta = 0^\circ$ (the orientation about y), the three-dimensional workspaces obtained at $\alpha = 0^\circ$, $+3^\circ$ and -3° (the orientation about z) are illustrated in Figs. 11(a)–(c), respectively.

As shown in Figs. 10 and 11, it is realized that the force-closure workspace is always smaller than and inside the convex hull formed by the base. This is useful to set the initial possible displacement ranges for discretizing. Moreover, with $\gamma = \beta = 0^\circ$, the 8-6-CDSPM looked from the top is actually equivalent to the 4-3-CDPPM. Therefore, the cross sections of the three-dimensional workspaces in Fig. 11 are exactly the same as the two-dimensional workspaces in Fig. 10 due to their similar dimensions.

From the previous illustrations, it can be seen that the recursive algorithm can be generally applied to completely restrained positioning mechanisms and redundantly restrained positioning mechanisms. These results can be verified through the null space approach—the homogeneous solution of underdetermined linear systems [9].

5. Conclusion

The general algorithm to generate the force-closure workspace of cable-driven parallel mechanisms is the major subject of this paper. A set of discrete postures which satisfy the force-closure condition constitutes the force-closure workspace. The recursive algorithm has been applied successfully to check the force-closure and then generate the workspace of a 4-3-CDPPM, which is a completely restrained positioning mechanism, and a 8-6-CDSPM, which is a redundantly restrained positioning mechanism. Due to the generic formulation approach, the proposed algorithm can be used for both completely restrained positioning mechanisms ($m = n + 1$) and redundantly restrained positioning mechanisms ($m > n + 1$). As the computational resolution is increased, the resulted workspaces are more precise.

As discussed in Section 3.2 the convex hull can also be visualized if the task-space dimension is less than or equal to three. However, this geometrical visualization becomes ineffective as the number of cables increases because of the convex hull formulation. On the other hand, the proposed algorithm can still be applied for incompletely restrained positioning mechanisms ($m < n + 1$) by combining external forces and cable tensions instantaneously. In brief, this approach can be generally used to create the force-closure workspace for various cable-driven parallel mechanisms.

Acknowledgements

The authors would like to thank the School of Mechanical and Aerospace Engineering at Nanyang Technological University for sponsoring this research program.

Appendix A. Force-closure checking steps of examples in Fig. 6

The sequential procedures to check the convex hull (or force-closure) for sample cases in Fig. 6 are shown in Figs. A.1 and A.2. In Fig. A.1, both positive and negative components exist in each

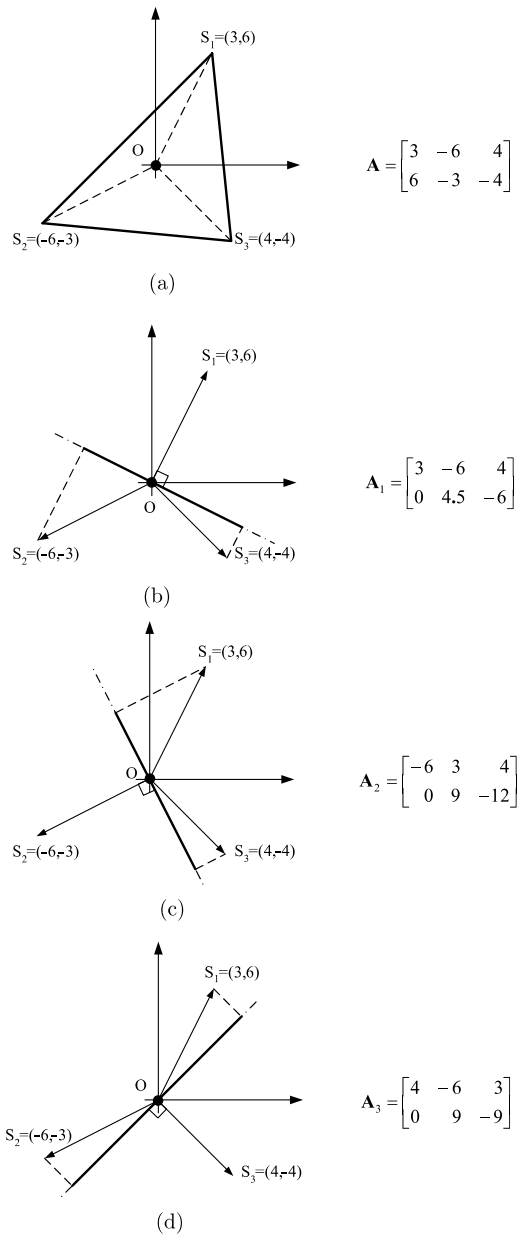


Fig. A.1. (a) The original structure matrix. (b) Step 1: The signs are changed in the second row. (c) Step 2: The signs are changed in the second row. (d) Step 3: The signs are changed in the second row. Computational steps for the case in Fig. 6(a).

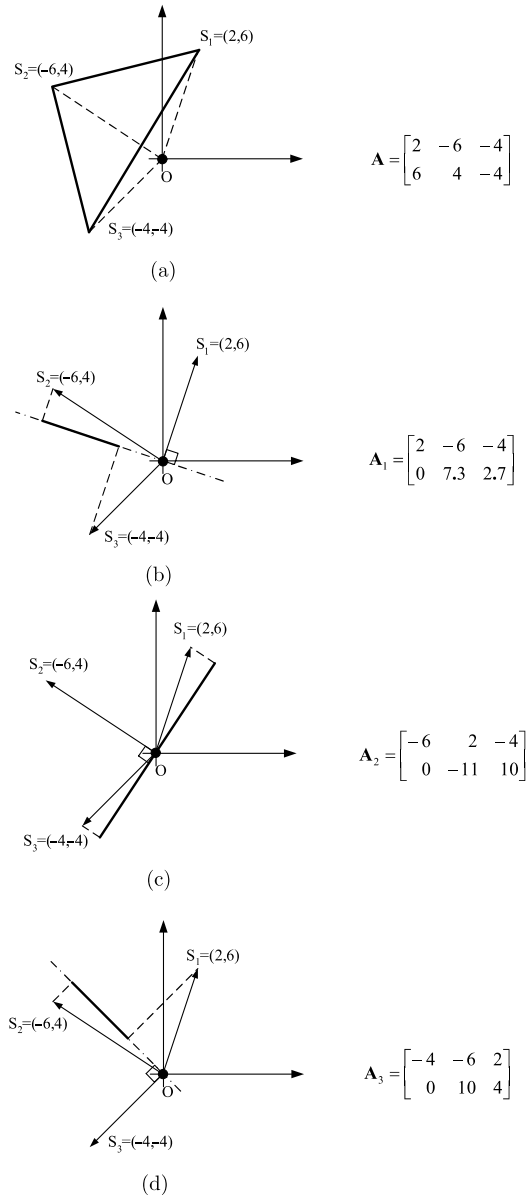


Fig. A.2. (a) The original structure matrix. (b) Step 1: The signs are the same in the second row. (c) Step 2: The signs are changed in the second row. (d) Step 3: The signs are the same in the second row. Computational steps for the case in Fig. 6(b).

sub-matrix (the second row), whereas there exists at least one sub-matrix which composes all negative or all positive components as seen in Fig. A.2.

References

- [1] L.W. Tsai, *Robot Analysis—The Mechanics of Serial and Parallel Manipulators*, A Wiley-Interscience Publication, 1999.
- [2] J. Albus, R. Bostelman, N. Dagalakis, The nist robocrane, *Journal of Robotic Systems* 10 (5) (1993) 709–724.
- [3] J.W. Jeong, S.H. Kim, Y.K. Kwak, C.C. Smith, Development of a parallel wire mechanism for measuring position and orientation of a robot end-effector, *Journal of Mechatronics* 8 (1998) 845–861.
- [4] E. Ottaviano, M. Ceccarelli, M. Toti, C.A. Carrasco, Catrasys (cassino tracking system): A wire system for experimental evaluation of robot workspace, *Journal of Robotics and Mechatronics* 14 (1) (2002) 78–87.
- [5] P. Lafourcade, M. Llibre, Design of a parallel wire-driven manipulator for wind tunnels, in: *Proceedings of the Workshop on Fundamental Issues and Future Research Directions for Parallel Mechanisms and Manipulators*, Quebec City, Canada, October 3–4 2002, pp. 187–194.
- [6] T. Morizono, K. Kurahashi, S. Kawamura, Realization of a virtual sports training system with parallel wire mechanism, in: *Proceedings of IEEE Conference on Robotics and Automation*, Albuquerque, New Mexico, April 1997, pp. 3025–3030.
- [7] R.L. Williams II, Cable-suspended haptic interface, *Journal of Virtual Reality* 3 (3) (1998) 13–21.
- [8] K. Homma, O. Fukuda, Y. Nagata, Study of a wire-driven leg rehabilitation system, in: *Proceedings of IEEE/RSJ International Conference on Intelligent Robots and Systems*, Lausanne, Switzerland, October 2002, pp. 1451–1456.
- [9] A. Ming, T. Higuchi, Study on multiple degree-of-freedom positioning mechanism using wires (part 1)—concept, design and control, *International Journal of Japan Social Engineering* 28 (2) (1994) 131–138.
- [10] S. Tadokoro et al., A motion base with 6-dof by parallel cable drive architecture, *IEEE/ASME Transactions on Mechatronics* 7 (2) (2002) 115–123.
- [11] S. Tadokoro et al., On fundamental design of wire configurations of wire-driven parallel manipulators with redundancy, in: *Japan/USA Symposium on Flexible Automation*, vol. 1, 1996, pp. 151–158.
- [12] C.M. Gosselin, G. Barrette, Kinematic analysis of planar parallel mechanisms actuated with cables, in: *Proceedings of Symposium on Mechanisms, Machines and Mechatronics*, Quebec, Canada, June 1 2001, pp. 41–42.
- [13] J. Pusey, A. Fattah, S. Agrawal, E. Messina, Design and workspace analysis of a 6-6 cable-suspended parallel robot, *Journal of Mechanism and Machine Theory* 39 (2004) 761–778.
- [14] R. Verhoeven, M. Hiller, S. Tadokoro, Workspace, stiffness, singularities and classification of tendon-driven stewart platforms, in: *International Symposium on Advances in Robot Kinematics*, Strobl, Austria, 1998, pp. 105–114.
- [15] R. Verhoeven, M. Hiller, S. Tadokoro, Workspace of tendon-driven stewart platforms: Basics, classification, details on the planar 2-dof class, in: *International Conference on Motion and Vibration Control MOVIC*, vol. 3, 1998, pp. 871–876.
- [16] R. Verhoeven, M. Hiller, Estimating the controllable workspace of tendon-based stewart platforms, in: *Proceedings of the International Symposium on Advances in Robot Kinematics*, Portoroz, Slovenia, 2002, pp. 277–284.
- [17] I. Ebert-Uphoff, P.A. Voglewede, On the connections between cable-driven robots, parallel manipulators and grasping, in: *Proceedings of IEEE Conference on Robotics and Automation*, New Orleans, LA, April 26–May 01 2004, pp. 4521–4526.
- [18] P. Bosscher, I. Ebert-Uphoff, Wrench-based analysis of cable-driven robots, in: *Proceedings of IEEE Conference on Robotics and Automation*, New Orleans, LA, April 26–May 01 2004, pp. 4950–4955.
- [19] H. Osumi, Y. Utsugi, M. Koshikawa, Development of a manipulator suspended by parallel wire structure, in: *Proceedings of IEEE/RSJ International Conference on Intelligent Robots and Systems*, Takamatsu, Japan, December 30–November 5 2000, pp. 498–503.
- [20] J.J. Craig, *Introduction to Robotics—Mechanics and Control*, Addison-Wesley Publishing Company, 1986.
- [21] R.T. Rockafellar, *Convex Analysis*, Princeton University Press, 1970.